Molecular treatment of charge transfer in Li$^+$ + Ca collisions

M. Kimura, H. Sato, and R. E. Olson

Department of Physics, University of Missouri—Rolla, Rolla, Missouri 65401

The perturbed-stationary-state method, appended with electron translation factors, has been applied to charge transfer in Li$^+$ + Ca collisions for energies from 0.1 to 20 keV/amu. The Born-Oppenheimer wave functions and eigenvalues were generated using the pseudopotential technique, which reduced the many-electron system to a simpler two-electron problem. The molecular ground-state $X\,^1\Sigma^+$ is calculated to be bound and has the potential-well parameters $R_e = 6.20a_0$, $D_e = 1.11$ eV, $\omega_e = 235$ cm^{-1}, and $B_e = 0.263$ cm^{-1}. From the scattering computations, a representative value for the charge-transfer cross section is 4×10^{-15} cm^2 at 5 keV/amu. The cross section decreases rapidly as the energy is reduced below 1 keV/amu. At all energies studied, the dominant electron-capture reaction product is the ground-state Li atom.

INTRODUCTION

Charge transfer in ion-atom collisions in the low to intermediate energy range has been the subject of the extensive theoretical studies. Recently, coupled-state approaches have been developed within molecular[1-5] and atomic[6,7] frameworks. These methods have been developed both with and without the inclusion of the electron translation factors (ETF's).

The importance of ETF's in the molecular treatment, i.e., the perturbed-stationary-state (PSS) theory, of slow ion-atom collisions has been established through its application to several one-electron two-nuclei systems.[1-5] However, the choice of the so-called switching function, which is used in the ETF, is still open to question.[3,4,8,9] Surprisingly, only recently have the formal considerations of implementing ETF's in many-electron systems been considered.[10,11]

To date, the application of ETF's in the PSS formalism has been restricted to *one-electron* (or pseudo-one-electron) systems. A recent investigation of a two-electron system using the PSS theory has been reported.[12] This study, which neglects ETF's, illustrates the large variations in the cross sections that can arise from different choices of the electronic coordinate for the coupling matrix element evaluations. Thus it is necessary to extend the theoretical treatment to more complicated molecular systems where the effects of electron correlation are important.

One set of possible charge transfer reactions is collisions of alkali-metal ions with alkaline-earth atom targets. These reactions are pseudo-two-electron systems which are amenable to molecular calculations. Also, experiments are underway[13] that will directly test the numerical results, with the first system to be studied being

$$\text{Li}^+ + \text{Ca} \rightarrow \text{Li} + \text{Ca}^+ \ . \tag{1}$$

In this paper we will present calculated cross sections for process (1) in the energy range of 0.1—20 keV/amu. An eight-channel impact parameter PSS approach with ETF's has been employed. The details of the calculations follow in the next sections.

MOLECULAR STATES

In the present collision system, the two valence electrons in LiCa$^+$ determine the collision dynamics. By employing the pseudopotential technique which replaces the "core" electron interactions by some analytical potential, this many-electron system can be reduced to a relatively simple two-electron problem. This two-electron problem can then be solved by conventional methods to generate eigenfunctions and eigenvalues.

We have adopted the pseudopotential method developed by Bardsley and colleagues[14] to generate eigenfunctions and energies. We used a pseudopotential of the Gaussian form given by

$$V(\vec{r}) = \sum_{l,m} A_l e^{-\xi r^2} \, |\, l,m \, \rangle \langle \, l,m \, | \ - \frac{\alpha_d}{2(r^2 + d^2)^2}$$

$$- \frac{\alpha_q}{2(r^2 + d^2)^3} - \frac{Z_{\text{eff}}}{r} \ , \tag{2}$$

where A_l and ξ_l are l-dependent parameters, while α_d, α_q, and d are the dipole, and quadrupole polarizabilities, and the cutoff distance, respectively. Atomic units are used unless otherwise stated. This subject has been reviewed extensively by Bardsley[15] and to a lesser extent in our previous paper[2]; therefore, we will not repeat the discussion here. The pseudopotential parameters employed in the calculations are given in Table I. The Li parameters are from Bardsley.[15] The A_l and ξ_l values for Ca were determined from a fit to spectroscopic data while the dipole and quadrupole polarizabilities were taken from the review by Dalgarno.[16]

A Born-Oppenheimer potential energies $\epsilon_i(R)$ and eigenfunctions $\phi_i^{\text{BO}}(\vec{r};R)$ for an electronic Hamiltonian which contains the pseudopotential satisfies Schrödinger's equation

$$H_{\text{el}} \phi_i^{\text{BO}}(\vec{r};R) = \epsilon_i(R) \phi_i^{\text{BO}}(\vec{r};R) \ . \tag{3}$$

We adopted Slater-type orbitals (STO's) χ_m for basis functions. The orbital exponents of the STO's employed in the LiCa$^+$ calculation are given in Table II. The Li

TABLE I. Pseudopotential parameters (in a.u.).

	Li	Ca
A_0	+ 6.013 668	+ 14.657 839
A_1	−0.740 679	+ 5.431 091
A_2	−0.067 342	−7.228 347
ξ_0	+ 1.293 213	+ 0.962 201
ξ_1	+ 1.410 279	+ 0.565 376
ξ_2	+ 0.8	+ 1.070 192
d	0.75	1.40
α_d	0.192 5	3.65
α_q	0.112	0.74

atom basis set was taken from the work of Stevens et al.,[17] while the Ca basis set was from Liu and Olson.[18] A full configuration interaction method has been used to obtain solutions to Eq. (3). Within the limitations of our basis set, all two-electron configuration interactions were accounted for. We employed 129 and 96 configurations for the Σ and Π state calculations, respectively. The importance of correlation is illustrated in the fact that a complete Hartree-Fock calculation for the ionization potential of Ca yields a value of 5.32 eV, which compares poorly to the spectroscopic value of 6.11 eV.

The Slater determinants are constructed from the STO's, not from molecular orbitals,

$$\Phi_n = |\, X_{mS}(\vec{r}_1)\mathscr{S}(\sigma_1)X_{m'S'}(\vec{r}_2)\mathscr{S}(\sigma_2)\,| \ , \quad (4)$$

where S and S' denote nucleus A or B as the origin of the atomic orbital, and $\mathscr{S}(\sigma_i)$ represents the spin function. The Born-Oppenheimer wave function is expressed as a linear combination of the Slater determinants as

$$\phi_i^{BO}(\vec{r};R) = \sum_n C_{ni}\Phi_n \ . \quad (5)$$

TABLE II. Orbital exponents of Slater-type—orbital basis functions.

Li 1s	0.412	
Li 2s	1.610	
	0.732	
	0.300	
Li 2p	2.013	
	0.501	
Ca 4s	3.091	
	1.629	
	1.012	
	0.667	
Ca 4p	1.094	
	0.698	
Ca 3d	2.122	
	0.801	

The energies $\epsilon_i(R)$ and coefficients C_{ni} are determined by the usual variational method. Calculated potential energy curves for the low-lying singlet Σ and Π molecular states of LiCa$^+$ are shown in Fig. 1. The triplet molecular states are not required to describe collision process starting from the Li$^+$ + Ca ground level. The potential-well parameters of the ground state $X^1\Sigma^+$ are calculated to be $R_e = 6.20a_0$, $D_e = 1.11$ eV, $\omega_e = 235$ cm^{-1}, and $B_e = 0.263$ cm^{-1}.

COUPLED EQUATIONS

It has been known for some time that the PSS theory does not satisfy Galilean invariance. Therefore, one obtains different results depending upon whether the origin for the electronic coordinate is chosen to be on the projectile, the target, or at the center of mass. This ambiguity leads to an origin dependence in the calculated matrix elements and the cross sections. Formally, this deficiency has been remedied by introducing the ETF's in the expansion of the scattering wave function. The ETF modified PSS theory satisfies the scattering boundary conditions and therefore, leads to cross sections, which are independent of the choice of origin of the electronic coordinates. For a many-electron system, however, it has been stressed[19,20] that formal difficulties exist in including ETF's in the scattering wave function. However, if the Born-Oppenheimer wave function is expressed in terms of atomic orbitals, it is possible to circumvent the formal problems.

As a starting point, we have used the formal theory of slow ion-atom collisions described by Delos and Thorson.[11] The theory is extended to the two-electron system. Assuming that the heavy particle motion is described by a classical trajectory, the Schrödinger equation for the electrons is given by
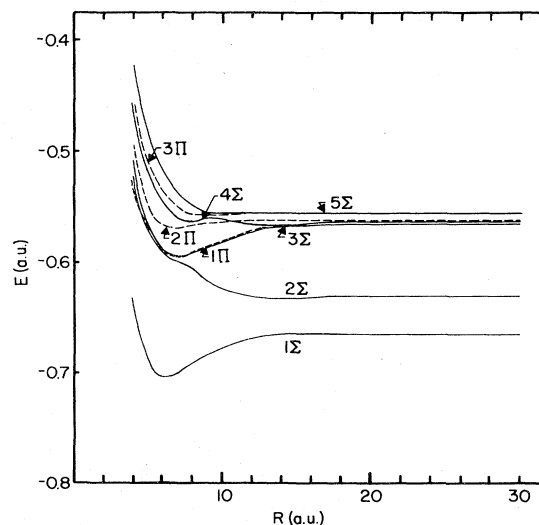

FIG. 1. Adiabatic potential energy curves for the singlet molecular states of LiCa$^+$. Solid lines denote $^1\Sigma$ states and dashed lines $^1\Pi$ states.

$$i\frac{\partial}{\partial t}\psi = H_{el}\psi \ . \tag{6}$$

Expanding the scattering wave function in terms of Born-Oppenheimer wave functions which incorporate ETF's, one obtains

$$\psi = \sum_i a_i(t)\phi_i^{BO}(\vec{r};R)F_i \ , \tag{7}$$

where F_i represents the molecular ETF which has the form

$$F_i = \exp\left[i\sum_k \left[\tfrac{1}{2}f_i(\vec{r}_k;R)\vec{V}\cdot\vec{r}_k - \tfrac{1}{8}\int^t V^2 dt'\right]\right] \ . \tag{8}$$

In Eq. (8), $\vec{V}$ is the relative velocity of the two heavy particles and f_i is a state-dependent switching function employed to represent a local propagation velocity of the electron in the quasimolecule formed during the collision. The detailed definition and proposed form of the switching function may be found in Ref. 10.

Substituting Eq. (7) into Eq. (6), multiplying by $\phi_j^* F_j^*$ from the left, and expanding the ETF in terms of $\vec{V}$, and also integrating over the electronic coordinates, we obtain the appropriate coupled equations. Retaining terms to first order in $\vec{V}$ yields

$$i\dot{a}_j = \epsilon_j a_j + \sum_i \vec{V}\cdot(\vec{P}+\vec{A})_{ji}a_i \ , \tag{9}$$

where

$$\vec{P}_{ji} = -i\langle\phi_j^{BO}\,|\,\vec{\nabla}_R\,|\,\phi_i^{BO}\rangle \ , \tag{10}$$

$$\vec{A}_{ji} = -i\left\langle\phi_j^{BO}\left|\sum_k (\vec{\nabla}_k\cdot\vec{S}_i^k)\cdot\vec{\nabla}_k + \tfrac{1}{2}(\nabla_k^2\vec{S}_i^k)\right|\phi_i^{BO}\right\rangle \ , \tag{11}$$

and

$$\vec{S}_i^k = \tfrac{1}{2}f_i(\vec{r}_k;R)\vec{r}_k \ . \tag{12}$$

Equations (10) and (11) are termed the nonadiabatic coupling matrix $\vec{P}$ and its ETF correction matrix $\vec{A}$, respectively. In a rotating coordinate frame the ETF corrected nonadiabatic coupling terms of Eq. (9) are divided into two contributions

$$\vec{V}\cdot(\vec{P}+\vec{A}) = \dot{R}(P+A)^R + \dot{\theta}(P+A)^\Theta \ . \tag{13}$$

The first term corresponds to radial coupling and the second to angular (rotational) coupling.

We have expanded the Born-Oppenheimer wave function in terms of Slater determinants of atomic orbitals equations (4) and (5). The wave function ϕ_j^{BO} can be rewritten as the product of

$$\sum_M u_{Mj}\chi_{mS}(\vec{r}_1)\chi_{m'S'}(\vec{r}_2) \tag{14}$$

and the spin part, where the collective index M denotes m,S,m',S'. Substituting Eq. (14) into Eqs. (10) and (11), we obtain

$$\vec{P}_{ji} = -i\sum_M\sum_N [u_{Mj}^*(\vec{\nabla}_R u_{Ni})\langle\chi_{mS}\,|\,\chi_{nT}\rangle\langle\chi_{m'S'}\,|\,\chi_{n'T'}\rangle + u_{Mj}^* u_{Ni}(\langle\chi_{mS}\,|\,\vec{\nabla}_R\,|\,\chi_{nT}\rangle\langle\chi_{m'S'}\,|\,\chi_{n'T'}\rangle$$

$$+\langle\chi_{mS}\,|\,\chi_{nT}\rangle\langle\chi_{m'S'}\,|\,\vec{\nabla}_R\,|\,\chi_{n'T'}\rangle)] \ , \tag{15}$$

and

$$\vec{A}_{ji} = -i\sum_M\sum_N u_{Mj}^* u_{Ni}[\langle\chi_{mS}\,|\,(\vec{\nabla}_k\cdot\vec{S}_i^k)\cdot\vec{\nabla} + \tfrac{1}{2}(\nabla_k^2\vec{S}_i^k)\,|\,\chi_{nT}\rangle\langle\chi_{m'S'}\,|\,\chi_{n'T'}\rangle$$

$$+\langle\chi_{mS}\,|\,\chi_{nT}\rangle\langle\chi_{m'S'}\,|\,(\vec{\nabla}_k\cdot\vec{S}_i^k)\cdot\vec{\nabla} + \tfrac{1}{2}(\nabla_k^2 S_i^k)\,|\,\chi_{n'T'}\rangle] \ . \tag{16}$$

Here, we assumed that

$$f_i(\vec{r};R)\chi_{nT}(\vec{r}) = \pm\chi_{nT}(\vec{r}) \ , \tag{17}$$

where the plus sign is taken when $T = A$ and the minus sign when $T = B$. Equation (17) corresponds to using atomic ETF's and is a reasonable assumption for large internuclear separations where the overlap between atomic orbitals of the two nuclei is small. With these assumptions, Eqs. (15) and (16) reduce to

$$(\vec{P}+\vec{A})_{ji} = -i\sum_M\sum_N \{u_{Mj}^*(\vec{\nabla}_R u_{Ni})\langle\chi_{mS}\,|\,\chi_{nT}\rangle\langle\chi_{m'S'}\,|\,\chi_{n'T'}\rangle$$

$$+u_{Mj}^* u_{Ni}[\langle\chi_{mS}\,|\,(\vec{\nabla}_R \pm \tfrac{1}{2}\vec{V})\,|\,\chi_{nT}\rangle\langle\chi_{m'S'}\,|\,\chi_{n'T'}\rangle + \langle\chi_{mS}\,|\,\chi_{nT}\rangle\langle\chi_{m'S'}\,|\,(\vec{\nabla}_R \pm \tfrac{1}{2}\vec{V})\,|\,\chi_{n'T'}\rangle]\} \ . \tag{18}$$

It can be shown that the coupling matrix elements, Eq. (18), are origin independent. The spurious long-range coupling in the term $\vec{P}$, which is troublesome in the PSS method, is canceled exactly by the term $\vec{A}$.

Since we used R-independent orbital exponents in the STO's, the second term of Eq. (18) does not contribute to the radial coupling. However, only the second term contributes to the angular coupling. Rewriting Eq. (18), one obtains

$$(\vec{P}+\vec{A})_{ji}^R = -i\sum_M\sum_N u_{Mj}^* \frac{du_{Ni}}{dR}\langle\chi_{mS}\,|\,\chi_{nT}\rangle\langle\chi_{m'S'}\,|\,\chi_{n'T'}\rangle \ , \tag{19}$$

and

$$(\vec{P}+\vec{A})_{ji}^{\Theta} = -i \sum_{M} \sum_{N} u_{Mj}^{*} u_{Ni} (\langle \chi_{mS} \mid il_{y}^{T} \mid \chi_{nT} \rangle \langle \chi_{m'S'} \mid \chi_{n'T'} \rangle + \langle \chi_{mS} \mid \chi_{nT} \rangle \langle \chi_{m'S'} \mid il_{y}^{T'} \mid \chi_{n'T'} \rangle) . \tag{20}$$

In Eq. (20), l_{y}^{T} is the perpendicular component of the electronic angular momentum relative to the collision plane about the nucleus T. For our application to the LiCa^{+} system, Eqs. (19) and (20) were employed in the calculations.

The method described above is exactly equivalent (to first order in V), to expanding the scattering wave function in terms of Born-Oppenheimer basis functions which incorporate atomic state ETF's. This method satisfies the boundary conditions and removes spurious long-range coupling terms arising from the PSS theory. The details of solving Eq. (9) and obtaining the cross section have already been fully described elsewhere and will not be duplicated here (Ref. 1).

As previously stated, we have retained only the first-order correction to the ETF's to obtain Eq. (9). Such an approximation is valid for collision velocities up to approximately the orbital velocity of the valence electrons, provided there is no region of strong coupling at large internuclear distances between the initial and charge transfer channels. In such cases, higher-order corrections must be retained to obtain accurate results. Fortunately, the LiCa^{+} system does not have such a long-range coupling region as can be seen by Figs. 1 and 2; the coupling is well localized at $R \leq 15a_{0}$. At higher collision velocities, corresponding to energies above 20 keV/amu, the first-order approximation becomes invalid leading to cross sections which overestimate the "true" values.

COUPLING MATRIX ELEMENTS

Calculated values for the dominant Σ-Σ radial coupling matrix elements are displayed in Fig. 2. The charge

transfer process is primarily determined by the radial coupling from the initial Li^{+} + Ca channel (1Σ) to the lowest-lying charge transfer state Li + Ca^{+} (2Σ). Both the 1$\Sigma$$\rightarrow$2$\Sigma$ and 2$\Sigma$$\rightarrow$1$\Sigma$ coupling terms are shown to display the non-Hermitian property of the matrix elements. Strong localized coupling between 1Σ and 2Σ occurs in the region of the maxima of the two matrix elements, $R \sim 12a_{0}$. Other maxima for 1$\Sigma$$\leftrightarrow$2$\Sigma$ occur at $R \simeq 6a_{0}$ which is attributed to the change of character of the 2Σ state due to strong mixing with the 3Σ level from Ca^{+} + Li*(2p). The 2$\Sigma$$\rightarrow$3$\Sigma$, 3$\Sigma$$\rightarrow$4$\Sigma$, and 4$\Sigma$$\rightarrow$5$\Sigma$ radial coupling terms display maxima due to avoided crossings between the respectively levels. These coupling terms play an important role in the sequential flux promotion to the higher levels.

All the angular coupling matrix elements that connect the 1Σ initial channel to the higher Π states are weak except in the small-R region where the 1$\Sigma$$\rightarrow$1$\Pi$ coupling term is significant. Owing to the impact parameter weighting in the cross-section determination, these terms are of secondary importance.

CROSS SECTIONS

A coupled-state calculation with eight molecular states (five Σ and three Π states) has been performed to obtain the partial cross sections. In order to interpret the collision mechanisms, we show in Fig. 3 the impact parameter times probability, $bP(b,E)$, versus the impact parameter b for charge transfer to the Li + Ca^{+} (2Σ) state at several collision energies. At low collision energies, $E \leq 1$ keV/amu, $bP(b,E)$ displays oscillatory structure which is characteristic of Demkov coupling.[21] As the collision en-
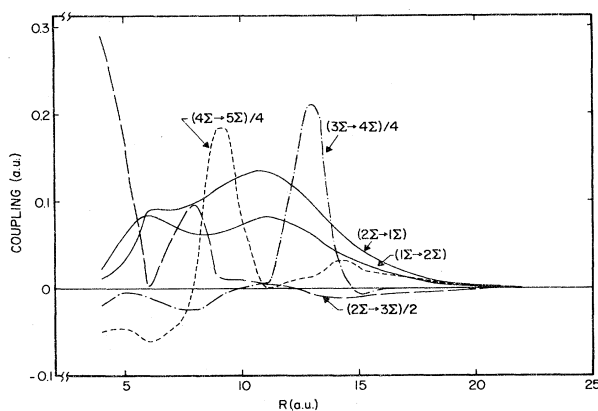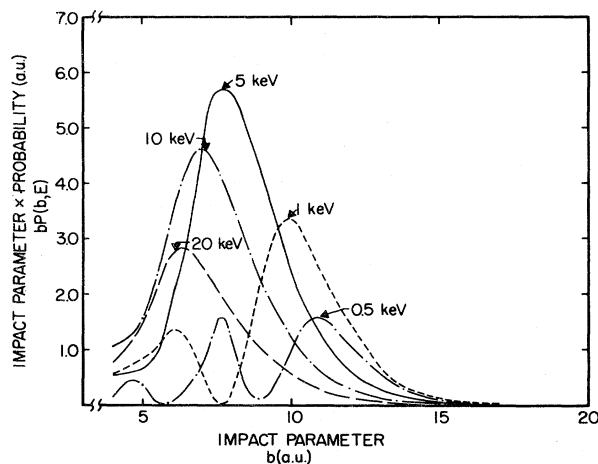

FIG. 2. Radial coupling matrix elements between the $^{1}\Sigma$ states. Both the forward- and backward-coupling terms are given for the dominant interaction between the 1Σ and 2Σ states.

FIG. 3. Transition probability to the Li + Ca^{+} charge transfer state times the impact parameter is plotted vs the impact parameter for several of the collision energies.

ergy increases, the oscillatory behavior of $bP(b,E)$ disappears since its frequency is proportional to v^{-1}. The location of the largest peak of $bP(b,E)$ at $b\simeq10a_0$ shifts toward smaller impact parameters as the collision energy increases. However, the magnitude of the peak reaches its maximum at 3—5 keV/amu. A time evolution study of the collision clearly indicates that the dominant inelastic channel is charge transfer to the $Li(2s)+Ca^+$ state through strong radial coupling with the initial channel $(1\Sigma\rightarrow2\Sigma)$. For small impact parameter collisions, a portion of the flux is promoted to the excited $Li^*(2p)+Ca^+$ charge transfer state directly due to strong angular coupling between the 1Σ and 1Π states. A small but nonnegligible portion of the flux goes to higher states which correspond to excitation of the Ca atom. The mechanism is sequential radial coupling and as a secondary effect, angular coupling. In Fig. 4, the calculated charge transfer cross sections for production of the $Li(2s)+Ca^+$ and $Li^*(2p)+Ca^+$ states are presented. Also, the excitation cross section to $Li^++Ca(4s\,3d\,^1D)$ is shown. The energy range investigated was 0.1—20 keV/amu.

Because of the strong radial coupling between the 1Σ and 2Σ states, charge transfer to $Li(2s)+Ca^+$ dominates over the entire energy region. The electron capture cross section to the $Li^*(2p)$ excited state shows a trend similar to that of the $Ca(4s\,3d\,^1D)$ excitation until ~10 keV/amu. Above this energy, there is a slight difference in the energy dependence of the two cross sections.

To check the convergence of the cross section, we have also performed two-state calculations employing the 1Σ and 2Σ molecular states. The differences between the two-state and the eight-state cross sections are small, only 3% and 11% at 1 and 10 keV/amu, respectively. Qualitatively, the two-state calculation provides reasonably accurate results over the entire energy region studied.

At this moment, we are unable to compare our results with the experimental measurements, since none are available. Thus it is difficult to assess the accuracy of the calculation. However, from consideration of the deficiencies in our theoretical treatment, we conclude that the total charge transfer cross section may be too small by up to 30%. The errors arise from two sources related to the calculation of the molecular states. The first is that the pseudopotential method fails at small internuclear separations $(R\leq3a_0)$ when the cores begin to overlap. The neglect of this region will give rise to a calculated cross section that is too small at high energies due to the lack of completely
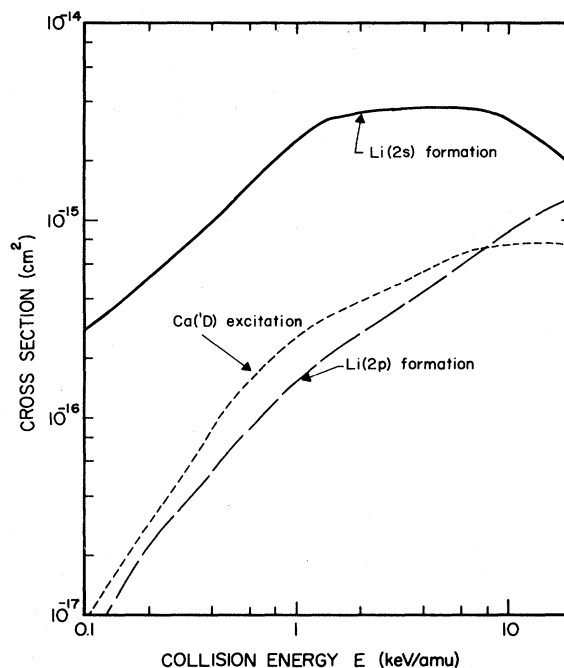

FIG. 4. Partial cross sections for the charge transfer products $Li(2s)+Ca^+$ and $Li^*(2p)+Ca^+$ and excitation of the target, $Li^++Ca(4s\,3d\,^1D)$.

including the angular coupling on the repulsive wall of the potentials. The other deficiency is related to the finite size of the basis set and the two-electron correlation problem. Although all the molecular states asymptotically dissociate to the spectroscopic separated atom limits to within 0.003 a.u., the calculated ΔE between the two lowest $^1\Sigma$ states is too large by 20% ($\Delta E_{spect}=0.026$ a.u.). This difference will lead to an underestimate of the cross sections, particularly in the threshold region.

[1]M. Kimura and W. R. Thorson, Phys. Rev. A **24**, 1779 (1981); **24**, 3014 (1981).
[2]M. Kimura, R. E. Olson, and J. Pascale, Phys. Rev. A **26**, 3113 (1982).
[3]T. A. Green, Phys. Rev. A **23**, 519 (1981); **23**, 532 (1981).
[4]G. J. Hatton, N. F. Lane, and T. G. Winter, J. Phys. B **12**, 571 (1979).
[5]T. G. Winter and G. J. Hatton, Phys. Rev. A **21**, 793 (1980).
[6]W. Fritsch and C. D. Lin, Phys. Rev. A **26**, 762 (1982).
[7]B. H. Bransden and C. J. Noble, J. Phys. B **15**, 451 (1982).
[8]W. R. Thorson, M. Kimura, J. Choi, and S. K. Knudson, Phys. Rev. A **24**, 1768 (1981).
[9]J. Vaaben and K. Taulbjerg, J. Phys. B **14**, 1815 (1981).
[10]J. B. Delos, Rev. Mod. Phys. **53**, 287 (1981).

[11]J. B. Delos and W. R. Thorson, J. Chem. Phys. <u>70</u>, 1774 (1979).

[12]A. Macias, A. Riera, and M. Yanez, Phys. Rev. A <u>23</u>, 2941 (1981).

[13]M. J. Coggiola (private communication).

[14]J. N. Bardsley, B. R. Junker, and D. W. Norcross, Chem. Phys. Lett. <u>37</u>, 502 (1976).

[15]J. N. Bardsley, Case Stud. At. Phys. <u>4</u>, 299 (1974).

[16]A. Dalgarno, Adv. Phys. (G.B.) <u>11</u>, 281 (1962).

[17]W. J. Stevens, A. M. Karo, and J. R. Hishes, J. Chem. Phys. <u>74</u>, 3989 (1981).

[18]B. Liu and R. E. Olson, Phys. Rev. A <u>18</u>, 2498 (1978).

[19]A. Riera and A. Salin, J. Phys. B <u>9</u>, 2877 (1976).

[20]A. Salin, Comments At. Mol. Phys. <u>9</u>, 165 (1980).

[21]R. E. Olson, Phys. Rev. A <u>6</u>, 1822 (1972).